

Adsorption of Freons by calcium carbonate under atmospheric conditions

V.S. Zakharenko and A.N. Moseichuk¹

*G.K. Boreskov Institute of Catalysis,
Siberian Branch of the Russian Academy of Sciences, Novosibirsk*
¹*Institute of Petroleum Chemistry,
Siberian Branch of the Russian Academy of Sciences, Tomsk*

Received February 2, 2005

The process of interaction of halogen-containing organic compounds (Freons: 134a, 22, and 12) with calcium carbonate surface under illumination and conditions close to the tropospheric ones was studied. It is suggested that the interaction is a destructive photosorption of Freons (134a or 22). This interaction yields the surface calcium fluoride and calcium chloride. The spectral dependence of the effective quantum yield for Freon 134a is determined.

Introduction

In the atmospheric layer closest to the Earth's surface – troposphere, various processes occur, which yield a decrease in the concentrations of gaseous atmospheric pollutants. The main process is the mixing by airflows that causes the dilution of a pollutant. The processes leading to cleaning of the ambient air include also the gas-phase (*homogeneous*) chemical reactions of pollutant oxidation by strong oxidants, for example, ozone or atomic oxygen formed from ozone under the solar irradiation.^{1,2}

Heterogeneous processes involve the adsorption of gas molecules by the Earth's surface, vegetation, inner and outer surfaces of buildings and constructions, as well as the absorption of molecules by water of rivers, lakes, seas, and oceans.³ *Heterogeneous* processes (interfaces: gas – liquid aerosol, gas – solid aerosol) can also result in removal of pollutants from the gas atmosphere. For example, such processes clean the air during rains (absorption process), snowfall, and dust storms (adsorption process).

Adsorption on the surface of aerosol particles occurs due to their permanent residence in the troposphere till the establishment of the adsorption (absorption) equilibrium, determined by the concentration of a pollutant in the gas phase and the adsorptivity of solid aerosol particles or their solubility in the liquid aerosol.

It is known from the experimental data that the elemental composition of solid aerosol particles in the troposphere is qualitatively⁴ (and even quantitatively for many elements) close to that of the lithosphere.⁵ Chemical compounds comprising the tropospheric solid aerosol include calcium carbonate (minerals of the carbonate class: calcite and aragonite). For example, in the solid aerosol collected from the ambient air onto a filter, the content of calcium carbonate achieves 10 weight percent of the total amount.⁶

We have investigated the dark and light-induced adsorption of Freons 12 (CF₂Cl₂), 22 (CHF₂Cl), and 134a (CF₃CH₂F) on samples of calcium carbonate prepared using different methods. For comparison, some results obtained for samples of magnesium oxide, having high photosorption activity for Freons,⁷ are presented as well.

Technique

In this study, we used an industrial calcium carbonate sample (I) of very high purity grade with the specific surface ~0.2 m²/g (total surface of 0.2 m²), placed on the reactor bottom without pre-treatment. According to data of the X-ray phase analysis, this sample is calcite. Another sample of calcium carbonate (II) was produced from calcium oxide of high purity grade after preparing its aqueous suspension, putting it on the reactor wall, and keeping in air for a long time in the open reactor. The specific surface of calcium carbonate (II), prepared in this way, was 12 m²/g (total surface of 12 m²).

The reactor with an industrial sample of magnesium oxide of the reagent grade with the specific surface ~10 m²/g (total surface of 7 m²) was prepared in the same way.

After soldering to a high-vacuum system, the reactors with samples were pumped out at a room temperature to decrease the rate of CO₂ escape from the sample surface. For water in the reactor to be constant during the evacuation, CO₂ was pumped out through a trap with a freezing mixture. Once the trap was heated in the closed reactor volume to the room temperature, the water frozen in the trap was repeatedly adsorbed on the sample surface. Thus, water vapor was always present in the gas phase of the reactor content, while adsorbed water and carbon dioxide were always present on the sample surface. In this case, the composition of the adsorbed particle

layer in the reactor corresponds to the composition of the adsorbed layer of particles of tropospheric solid aerosol, consisting, for example, of calcite (CaCO_3) or periclase (MgO) particles.⁸

Freons 12 (CF_2Cl_2) and 134a ($\text{CF}_3\text{-CH}_2\text{F}$) were produced by the Scientific Center "Prikladnaya Khimiya" (St. Petersburg). Freon 22 (CHF_2Cl) was produced by the Ural Industrial Association "Galogen." All the compounds used were additionally purified by refreezing.

The amount of halogen-containing hydrocarbon (HCHC) in the reactor volume was calculated from the measurements of the total pressure in the reactor volume by a Pirani gage. The gas composition was determined by a monopolar mass spectrometer. The time scan in the scanning of the mass spectrum was 10 s, and the mass spectrum averaged over three scans was stored in the computer memory.

The amount of HCHC adsorbed in the dark was determined after the establishment of the pressure ~ 1 Pa in the reactor volume at the bypass of the known gas amount, previously pumped out through the trap with the freezing mixture (temperature of 180 K), from a measuring volume (100 cm^3) into the reactor volume (95 cm^3).

During the measurement of the amount of photosorbed HCHC, the pressure in the reactor volume (195 cm^3) was ~ 1 Pa. This pressure was selected because in the pressure range from 1 to 10^{-5} Pa the sensitivity of the pressure sensor (Pirani gage) is constant, and the partial pressure of Freons in the atmosphere does not exceed 10^{-2} Pa.

Whenever necessary, the composition of gas mixtures (before, during, and after the dark sorption and photosorption of HCHC) in the reactor volume was determined using the condensation analysis by the melting peaks of gases condensed at the temperature of liquid nitrogen as the temperature increased from the liquid nitrogen temperature to the room one. The condensation analysis was accompanied by the mass-spectrometric analysis for identification of the melting peaks. The mass spectrometer in this process was operated either in the mode of scanning of several masses or in the mode of tuning to a supposed mass.

The main admixtures in HCHC used were atmospheric oxygen and nitrogen in the amount $< 1\%$ with regard to the main substance. During HCHC refreezing, oxygen and nitrogen were pumped out at the temperature of liquid nitrogen (77 K).

For the UV irradiation of the surface, we used an OSL-1 lighter of the luminescence microscopes with a DRSh-250 mercury lamp (250 W), a thermal water filter (quartz window and 5-cm thick water layer), and an UFS filter, whose transmission spectrum is shown in Fig. 1 (spectrum 1). The total density of the radiation flux, measured with an RTN-20S thermopile, was $\sim 1 \text{ mW/cm}^2$ for the UFS filter.

The intensity of the light flux and the area of the illuminated surface (geometric area was 14 cm^2) were maintained constant for all the samples and HCHC used in this work.

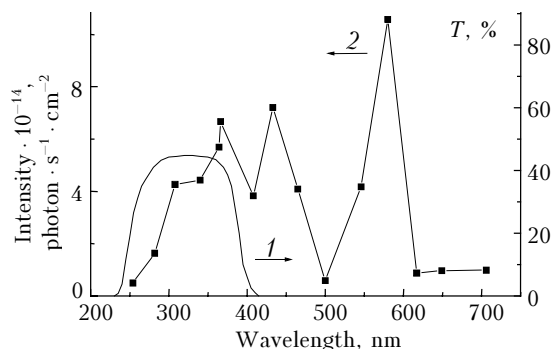


Fig. 1. Transmission spectrum (T) of the UFS glass filter used (1) and the spectrum of the net radiation passing through the front wall of the quartz reactor, measured with the interference filters (2).

The effective quantum yield of photosorption was defined as a number of photosorbed molecules to the number of quanta passed through the front wall of the reactor. Monochromatic radiation was separated out by interference filters. The intensity of the flux of quanta having passed through the front wall of the quartz reactor for these filters is shown in Fig. 1 (spectrum 2).

The diffuse reflection spectra in the IR region were recorded in air by an FTIR-8300 PC spectrometer manufactured by Shimadzu with the use of a DRS-8000 attachment before and after the experiments in the high-vacuum system. A mat metal surface served a reflection reference. The spectra were recorded as an average over 50 scans in a range of $400\text{--}6000 \text{ cm}^{-1}$ with the spectral resolution of 4 cm^{-1} . The obtained spectra were transformed into the Kubelka–Munk scale and represented as spectral dependence of the function

$$F(R) = (1 - R)^2/2R,$$

where R is reflection.

Results and discussion

Dark adsorption

The long exposure of the studied samples to air forms the state of their surface, at which the surface mostly adsorbs water (the water vapor concentration in the ambient air about 10^{17} cm^{-3}). Carbon dioxide and nitrogen oxides are adsorbed in smaller amounts (10^{15} cm^{-3} and 10^9 cm^{-3} , respectively). Water and carbon dioxide can be found in the composition of the gases desorbing from the surface of calcium carbonate samples after the evacuation of the reactor with the sample for 1 h at a room temperature. The gas composition corresponds to that of the gases escaped from the surface of magnesium oxide,⁹ but the amount of CO_2 and H_2O emitted by the unit surface of calcium carbonate is an order of magnitude smaller than by the unit surface of magnesium oxide.

The surface of MgO , kept in air for a long time and then put on the reactor wall by the technique described above, already contains almost a monolayer

of hydrogen-containing compounds (water, hydroxyl groups), ~10% of a monolayer of carbon-containing compounds (carbonates, CO₂, and CO), and up to 1% of a monolayer of nitrogen-containing compounds.⁹ The spectrum of the initial magnesium oxide sample is shown in Fig. 2 (spectrum 1); it corresponds to the above composition of the adsorbed layer of initial magnesium oxide.

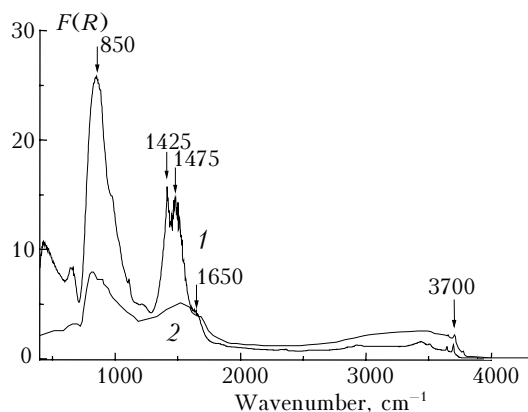


Fig. 2. Spectra of diffuse reflection in the IR region for initial MgO kept in air for a long time (1) and MgO heated in air at 773 K for 2 h (2).

The spectrum always includes the bands associated with the absorption by hydroxyl groups (3300–3800 cm⁻¹ [Ref. 10]), carbonates (1300–1800 cm⁻¹ [Ref. 11]), and nitrogen oxides (900–1200 cm⁻¹ [Ref. 12]). In the range of 750–900 cm⁻¹, an overtone is observed at 850 cm⁻¹, which corresponds to the 420 cm⁻¹ vibration of the magnesium oxide lattice.¹³ After heating of the initial magnesium oxide at 773 K for 2 h in air and cooling of the sample in air, the spectrum transforms into that shown in Fig. 2 (spectrum 2). In this spectrum, the intensities of carbonate absorption bands are much lower than the absorption intensity in the range corresponding to the absorption by hydroxyls.

In the dark, Freon 22 adsorbs on calcium carbonate samples, while no adsorption of Freons 12 and 134a is observed. Thus, the dark adsorption of Freon 22 on CaCO₃ (I) was 3.5% of a monolayer of the calcium carbonate surface, while its dark adsorption on magnesium oxide was 1% of a monolayer⁷ at the comparable total surfaces of the samples. The dark adsorption of Freon 22 on calcium carbonate samples has a partly reversible character, because adsorbed Freon is removed during the long evacuation at a room temperature.

The dark adsorption of Freon 22 on calcium carbonate samples occurs also in the case, if the dried air is present in the gas phase, and this can lead to a decrease of the Freon concentration in the ambient air.

Photosorption

The investigations into the interaction of gases with the surface of metal oxides under the effect of light quanta indicate that this interaction is either

photoadsorption of gases on surface centers^{14–16} or photosorption of gases, during which oxygen of the oxide lattice is substituted by halogen atoms from the molecules of the interacting gas.¹⁷ These two types of photoinduced processes are characterized not only by the different spectral dependences of the quantum efficiency (for the same metal oxide) and the values of surface filling by the gas adsorbed under the exposure to light, but also by different kinetics of the photoadsorption¹⁴ or photosorption.¹⁷

Thus, according to our data, the kinetics of photosorption of Freon 22, Freon 134a, and trichloroethane on MgO is described by first-order equations (Fig. 3, curves 1, 2 respectively for Freon 22 and Freon 134a). For MgO, the kinetics of photosorption of trichloroethane (Fig. 4, curve 1), as well as that of Freon 134a on calcium carbonate (Fig. 4, curve 2), is of the first order. Photosorption of Freon on calcium carbonate occurs before its transfer from the gas phase to a pressure of lower than 10⁻⁵ Pa, and the filling by photosorbed Freon can exceed 10% of a monolayer of the calcium carbonate surface.

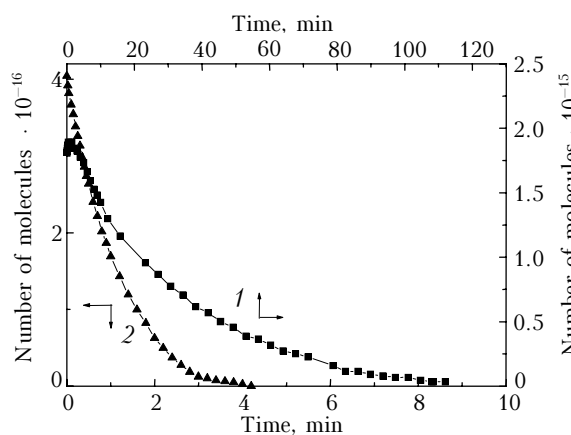


Fig. 3. Kinetics of photosorption of Freon 22 (1) and Freon 134a (2) on MgO. Temperature ~300 K, Freon 22 initial pressure of 1 Pa, and that of Freon 134a of 2 Pa.

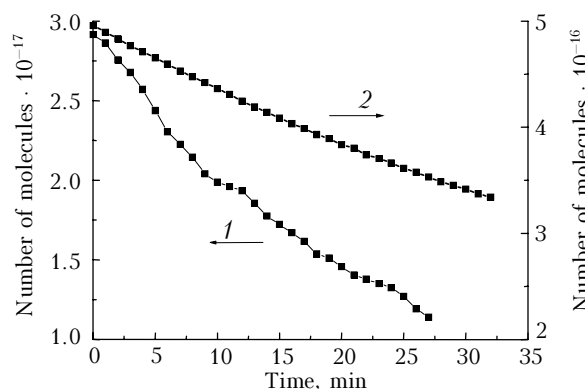


Fig. 4. Kinetics of photosorption of trichloroethane (1) on MgO surface and Freon 134a on CaCO₃ (II) (2). Temperature ~300 K, trichloroethane initial pressure of 4.6 Pa, and that of Freon 134a of 1 Pa.

The spectral dependence of the effective quantum yield of Freon photosorption on calcium carbonate is shown in Fig. 5.

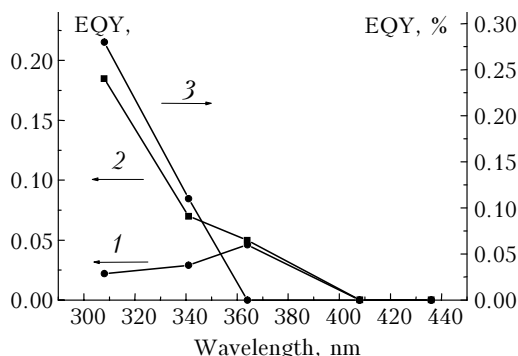


Fig. 5. Spectral dependence of the effective quantum yield (EQY) of photosorption of Freon 134a on CaCO_3 (II): after the 30 min irradiation by the net radiation of the DRS-250 mercury lamp in Freon 12 (1); after the additional 120 min irradiation by the net radiation in Freon 134a (2); photoadsorption of oxygen from the dried air (3).

The red boundaries of the photosorption spectra of Freon 134a for calcium carbonate (Fig. 5) and magnesium oxide¹⁸ coincide, which is likely connected with the formation of the adsorbed layer of their surfaces under the same conditions. It is worthy to note the increase of the quantum efficiency in the shortwave region (343 and 313 nm) for the photosorption of Freon 134a on CaCO_3 (II) after the additional irradiation of its surface in the atmosphere of Freon 134a by the net radiation of the mercury lamp (curves 1 and 2). This increase can be explained by a higher photosorption activity of calcium oxide, formed at the intermediate stage of transformation of calcium carbonate into calcium fluoride and chloride, in this spectral region. In this short-wave region, the photoadsorption of oxygen from the dried air on calcium carbonate samples is also observed (Fig. 5, curve 3) along with the photoadsorption of oxygen on calcium oxide after its high-temperature oxygen–vacuum treatment.¹⁹

Comparing the characteristics of photosorption of Freons on calcium carbonate and magnesium oxide samples, we can assume some analogy between the mechanisms of photosorption on these two compounds. First, for these two compounds, the formation of surface fluorides and chlorides of calcium and magnesium, respectively, is very probable. Second, the loss of surface oxygen from the lattice of calcium oxide (intermediate compound in the photosorption of Freon on calcium carbonate) and magnesium oxide to the oxidation of the Freon organic residue (formation of the C=O bond) is very probable.

This is also supported by the increase in the intensity of the bands corresponding to the carbonyl groups C=O, observed in the IR spectra; actually, in Fig. 6 one can see the increase of the intensity of absorption bands in a range of 1600–1700 cm^{-1} after the photosorption of Freon 134a on the MgO surface.

At the same time, it can be seen from Fig. 6 that, after the photosorption of Freon 134a on MgO in the

amount exceeding 10% of a monolayer of its surface, the intensity of IR absorption lines of C–F bonds (absorption spectra in the ranges of 1820–1870 and 2540–2640 cm^{-1}) is very low. This can also count in favor of the hypothesis that, under the exposure to light, the C–F bonds on the MgO surface break and the Mg–F bonds form in place of them. In the MgO spectrum after the photosorption of Freon 134a (Fig. 6), in contrast to the spectrum of the initial MgO sample (see Fig. 2), the intensity of the 1650 cm^{-1} band, corresponding to the absorption by bidentate carbonates, produced after the adsorption of carbon dioxide or monoxide on the hydroxylized MgO surface,^{8,19} is significantly increased. The intensity of absorption bands in a region of 3300–3800 cm^{-1} , corresponding to the absorption by hydroxyl groups,¹⁰ is also increased. A narrow band nearby 3700 cm^{-1} , according to the data of Ref. 20, corresponds to the absorption by isolated hydroxyl groups on the magnesium oxide surface and appears upon the irradiation of MgO by the UV radiation in the presence of hydrogen. The absorption in this spectral region decreases sharply after heating of magnesium oxide at 620 K in vacuum (see Fig. 6, spectrum 2) or in air (see Fig. 2, spectrum 2).

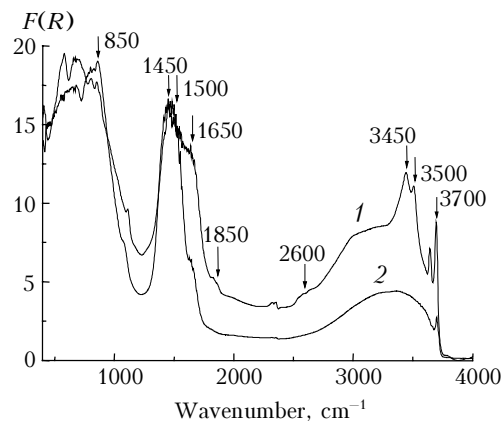


Fig. 6. Spectra of diffuse reflection in the IR spectral region for MgO after the photosorption of Freon 134a (1) and MgO heated at 620 K in vacuum (2).

Conclusions

Despite the high concentration of magnesium in the lithosphere (2 at. %), it is mostly present not as MgO, but in the form of magnesium sulfate and carbonate and some silicates. The main sources of magnesium oxide as a chemical phase component of solid aerosol particles are forest fires. The abundance of calcium carbonate as a phase is much higher – up to 10 weight percent already in the solid aerosol of the troposphere. Thus, regardless of the lower effective quantum yield (as compared to MgO) in the destructive photosorption of some halogen-containing hydrocarbons, the effect of calcium carbonate on the removal of such atmospheric pollutants is more significant than that of magnesium oxide.

Acknowledgments

The authors are grateful to E.A. Paukshtis for the help in recording of IR spectra and for the discussion of the results obtained.

This work was supported, in part, by the Grant No. 138 of the SB RAS Integration Project "Siberian Geospheric–Biospheric Program."

References

1. V.A. Isidorov, *Organic Chemistry of the Atmosphere* (Khimiya, St. Petersburg, 1992), 165 pp.
2. P.A. Leighton, *Photochemistry of Air Pollution* (Academic Press, New York, 1961), 320 pp.
3. P. Brimblecombe, *Air Composition and Chemistry* (Cambridge University Press, New York, 1986).
4. V.P. Baryshev, N.S. Bufetov, K.P. Koutzenogii, V.I. Makarov, and A.I. Smirnova, *Nucl. Instrum. and Meth. Phys. Res. A* **359**, 297–301 (1995).
5. G.A. Koval'skaya, *Atmos. Oceanic Opt.* **15**, Nos. 5–6, 458–462 (2002).
6. V.V. Malakhov, A.A. Vlasov, and L.S. Dovlitova, *Khimiya v Interesakh Ustoichivogo Razvitiya* **10**, No. 3, 643–650 (2002).
7. V.S. Zakharenko, A.N. Moseichuk, and V.N. Parmon, *Atmos. Oceanic Opt.* **15**, Nos. 5–6, 448–452 (2002).
8. I. Kostov, *Mineralogy* [Russian translation] (Mir, Moscow, 1971), 584 pp.
9. V.S. Zakharenko and V.N. Parmon, *Zh. Fiz. Khimii* **73**, No. 1, 124–127 (1999).
10. A.A. Davidov, A.A. Budneva, S.M. Aliev and V.D. Sokolovskii, *React. Kinet. Catal. Lett.* **36**, No. 2, 491–495 (1988).
11. Ya.M. Grigor'ev, D.V. Pozdnyakov, and V.N. Filimonov, *Zh. Fiz. Khimii* **46**, No. 2, 316–321 (1972).
12. L. Cerruti, E. Modone, E. Guglielminotti, and E. Borello, *J. Chem. Soc. Faraday Trans. I* **70**, No. 1, 729–739 (1974).
13. J. Fukuda and K. Tanabe, *Bull. Chem. Soc. Jap.* **46**, No. 6, 1616–1619 (1973).
14. L.L. Basov, V.A. Kotel'nikov, A.A. Lisachenko, V.L. Rapoport, and Yu.P. Solonitsyn, *Uspekhi Fotoniki* No. 1, 78–111 (1969).
15. M. Formenti and S.J. Teichner, *Catalysis (Specialist Periodical Reports)* **2**, 87–106 (1978).
16. M. Anpo, M. Che, B. Fubini, E. Garrone, E. Giamello, and M.C. Paganini, *Topics in Catal.* **8**, Nos. 3/4, 189–198 (1999).
17. V.N. Parmon and V.S. Zakharenko, *CatTech.* **5**, No. 2, 96–115 (2001).
18. V.S. Zakharenko, V.N. Parmon, and K.I. Zamaraev, *Kinet. i Katal.* **38**, No. 1, 140–144 (1997).
19. A.M. Volodin, A.E. Cherkashin, and K.N. Prokop'ev, *Kinet. i Katal.* **33**, No. 5, 1190–1195 (1982).
20. M. Sterrer, O. Diwald, and E. Knozinger, *J. Phys. Chem. B* **104**, No. 12, 3601–3607 (2000).